

Manuscript: GPPS-2018-0004

AN ENHANCED COMPRESSOR SUB-IDLE MAP GENERATION METHOD

Luis E. Ferrer-Vidal
Cranfield University
l.ferrer-vidal@cranfield.ac.uk
Cranfield, Bedfordshire, U.K.

Vassilios Pachidis
Cranfield University
v.pachidis@cranfield.ac.uk
Cranfield, Bedfordshire, U.K.

Richard J. Tunstall
Rolls Royce plc.
richard.tunstall@rolls-royce.com
Filton, Bristol, U.K.

ABSTRACT

Several techniques have come about for the mathematical extrapolation of compressor maps from the idle region down to zero speed. Relatively little work has been done on methods which attempt to extract compressor sub-idle performance from physical grounds. This paper focuses on the design of an axial compressor rig to obtain sub-idle data in the form of locked rotor and windmill characteristics. The rig design is presented and the results obtained discussed. The data gathered is used to generate physics-based sub-idle compressor maps which are then compared to existing methods for sub-idle map generation. Interpolation from the locked rotor characteristic is shown to improve map generation over extrapolation methodologies, while the windmilling characteristic is shown to be an important addition to the interpolation process.

INTRODUCTION

Idling is broadly defined as an operating condition where an engine is operating with no load applied. For the case of gas turbines, the idling speed is the minimum shaft speed required such that the engine may be maintained in stable operation, with the turbine load powering the auxiliaries and minimal net power produced. Sub-idle operation is then any operating regime where the shaft speed is below the idle speed (Walsh and Fletcher, 2004). While sub-idle operation may be of limited importance to the power industry, where gas turbine speed is matched to grid frequency and start-ups/shut-downs are relatively infrequent, operation below idle can have profound effects on aviation engines.

An aviation engine is exposed to the sub-idle regime on start-up or during windmill relight. While these events have historically not warranted a detailed performance evaluation, more stringent certification and customer requirements and the push for marginal benefits in fuel efficiency have highlighted the need for accurate sub-idle performance characterization (EASA, 2015). Additionally, modern engines with increasing by-pass ratios put a strain on relight capability, while gearboxes, driven accessories and larger engine masses also contribute to increased windmilling drag and reduced starting performance (Zachos, 2013). As the trend for higher by-pass ratios and geared configurations continues to increase, so too does the need for improved sub-idle performance.

Accurate performance prediction tools are an important part of the engine design process for meeting certification requirements on time and at a reduced research and development cost. Stringent end-user requirements on the relight capabilities of aviation engines mean that designers must be able to accurately predict the behavior of engine components during in-flight relight events. In addition, the drive towards improved efficiency and lower fuel burn means that the design for ground-starts and long taxi periods operating at low speed must be taken into account, increasing the need for performance optimization at and below idle. In order to use performance solvers to this effect, engine component maps for these cases must be available.

LITERATURE REVIEW

Sub-idle map generation

Compressor maps have traditionally been obtained from rig tests. Obtaining compressor maps in this manner for sub-idle regions is expensive and impractical, as a means to control the shaft torque while providing different mass flows to the engine would be required, instead of letting the engine set the flow upon operation (Illana, 2013). On the other hand, tools aimed at analytical map generation rely on component performance rules designed for nominal operation, with little knowledge available to predict sub-idle conditions. Due to this, many methods have been devised for the analytical extrapolation of sub-idle maps (Jones et al., 2001).

Map extrapolation has traditionally relied on a combination of graphical methods, past-experience, and engineering judgement (Kurzke, 1996). Such methods become problematic far below the idle speed, where limited data exists (Zachos et al., 2011). In order to calculate compressor starting behavior, Agrawal and Yunis (Agrawal and Yunis, 1982) devised a methodology making use of incompressible flow similarity relations to generate the start-up running line. Such approach was later expanded by Sexton (Sexton, 2001) to allow for the entire sub-idle map to be extrapolated.

The Sexton extrapolation method has been further developed by Gaudet and Gauthier showing promising results (Gaudet and Gauthier, 2007). This method extrapolates turbomachinery maps below the idle speed using relationships that take into account basic thermodynamic principles. Corrected mass flow, pressure ratio and efficiency are expressed in terms of the ratio of the sub-idle speed to a reference idle speed line:

$$\begin{aligned} \dot{m}_{corr_x} &= \dot{m}_{corr_{ref}} \times \left(\frac{N_x}{N_{ref}} \right)^p \\ \Pi_{0_x} &= \left(1 + \left(\left(\Pi_{0_{ref}} \right)^{\frac{\gamma-1}{\gamma}} - 1 \right) \times \left(\frac{N_x}{N_{ref}} \right)^q \right)^{\frac{\gamma}{\gamma-1}} \quad (1) \\ \eta_x &= \eta_{ref} \times \left(\frac{N_x}{N_{ref}} \right)^{(p+q)-r} \end{aligned}$$

Where the exponents p , q and r are defined by Gaudet and Gauthier using thermodynamic relations applied between the two lowest speed lines on the existing above-idle map (Gaudet and Gauthier, 2007):

$$\begin{aligned} p &= \frac{\log \left(\frac{\dot{m}_{corr_{ref+1}}}{\dot{m}_{corr_{ref}}} \right)}{\log \left(\frac{N_{ref+1}}{N_{ref}} \right)} \\ q &= \frac{\log \left(\frac{\left(\left(\Pi_{0_{ref}} \right)^{\frac{\gamma-1}{\gamma}} - 1 \right)_{ref+1}}{\left(\left(\Pi_{0_{ref}} \right)^{\frac{\gamma-1}{\gamma}} - 1 \right)_{ref}} \right)}{\log \left(\frac{N_{ref+1}}{N_{ref}} \right)} \quad (2) \\ r &= (p + q) - \frac{\log \left(\frac{\eta_{ref+1}}{\eta_{ref}} \right)}{\log \left(\frac{N_{ref+1}}{N_{ref}} \right)} \end{aligned}$$

This approach allows for a straight-forward analytical implementation of basic thermodynamic relations to quickly extrapolate the compressor maps below the idle speed. Such an analytical method is expected to have limitations as speed decreases and the compressor starts operating in stirrer and turbine modes, where the assumptions made in the derivation of the compressor relations no longer hold. As reviewed by Zachos et al. (Zachos et al., 2011), this methodology does not allow for pressure ratios below unity, failing to adequately capture the turbine operating mode of a compressor operating at speeds lower than windmilling.

In order to validate the extrapolation method at sub-idle speeds using experimental data, Honle et al. (Honle et al., 2013) extracted sub-idle data from an Allison M250-C20b axial-centrifugal compressor assembly. Pressure ratio and efficiency data were gathered down to 15% speed and compared to the results of the Gaudet extrapolation. Results showed good agreement of

pressure ratio data, while the efficiency extrapolation could not completely be validated against data at very low speeds. Honle et al. suggested the extrapolation methodology may be augmented using the method described by Aslanidou et al. (Aslanidou et al., 2010) and Zachos et al. (Zachos et al., 2011), but this was left as a future development.

The physically enhanced sub-idle map generation method presented in (Aslanidou et al., 2010) and (Zachos et al., 2011) relies on interpolation up to idle from an analytically generated locked rotor line, i.e. zero speed characteristic. This would enhance the method presented in (Gaudet and Gauthier, 2007) by allowing pressure ratios below unity and generating low speed lines which more closely resemble the physical operation of compressors operating below idle. Such a method has been used to generate compressor maps down to zero speed which capture the expected trends (Zachos et al., 2011) and have successfully been used in performance models (Grech, 2013), (Jia et al., 2016), but validation of the generated maps against experimental data is still required.

Sub-idle map representation

Compressor maps have traditionally been represented using the parameters of corrected shaft speed, corrected mass flow, pressure ratio, and isentropic efficiency. The use of corrected quantities ensures that Mach number similarity is maintained when environmental conditions differ from standard, as this is a main driver behind compressor performance (Farokhi, 2004).

$$\begin{aligned}
 \dot{m}_{corr} &= \frac{\dot{m} \sqrt{T/T_{ref}}}{\sqrt{P/P_{ref}}} \\
 N_{corr} &= \frac{N}{\sqrt{T}} \\
 \Pi_0 &= \frac{P_{tot2}}{P_{tot1}} \\
 \eta_{is} &= \frac{\Delta h_{is}}{\Delta h}
 \end{aligned} \tag{3}$$

However, as (Riegler, 2001) explained, the use of an efficiency parameter creates issues when in the sub-idle region, since the enthalpy addition becomes zero and isentropic efficiency becomes an undetermined quantity.

The use of linearized parameters such as flow coefficient (ϕ), work coefficient (ψ), and isentropic work coefficient (ψ_{is}) are also common for integration in several cycle decks (Grech, 2013).

$$\begin{aligned}
 \phi &= \frac{V_{ax}}{U} \\
 \psi &= \frac{\Delta h}{U^2} \\
 \psi_{is} &= \frac{\Delta h_{is}}{U^2}
 \end{aligned} \tag{4}$$

These linearized parameters have the benefit of reducing all compressor map information to a single line at low speeds, allowing compressor performance data to be stored in a more amicable format for computer algorithms. However, a parameter with shaft speed in the denominator will tend to infinity as blade speed goes to zero for a given value of velocity or enthalpy, invalidating the linearized map representation for sub-idle operation.

As explained by (Kurzke, 1996) and reviewed by (Grech, 2013), (Zachos, 2010), and (Howard, 2007), the representation of the map is not an issue as long as physical meaning is maintained. In order to bypass the difficulties mentioned above, (Riegler, 2001) and (Howard, 2007) have discussed the use of corrected shaft speed, corrected mass flow, and pressure ratio along with a torque parameter which is defined as:

$$\frac{\tau}{P_{in}} = \phi \times \psi \times \left(\frac{N}{\sqrt{T}} \right)^2 \times \frac{60}{2\pi} \tag{5}$$

Using this parameter solves the definition issue at sub-idle and, along with pressure ratio and corrected mass flow, has successfully been used by both (Zachos, 2010) and (Grech, 2013) to represent compressor maps down to zero speed. As such, the

parameters of corrected mass flow, corrected shaft speed, pressure ratio, and this torque parameter will be used in this work. This formulation was also successfully integrated by Grech into an existing performance code (Grech, 2013).

Windmilling for map generation

A linear relationship between windmilling mass flow and speed for the case of fans has been described in the literature (Binder et al, 2015), (Courty-Audren et al., 2013) (Prasad and Lord, 2004). Such a relationship has not yet been formally investigated for the case of multistage compressors. For the case of fans, this linear relationship means the windmilling regime can be represented by a single point on a $\phi - \psi$ linearized compressor map. The windmilling ϕ needs to be determined while $\psi = 0$ for windmilling with negligible friction. Methods to calculate the windmilling mass flow, speed and losses have been created for fans (Zachos, 2013), (Binder et al., 2015), allowing the windmill flow coefficient to be calculated for a known geometry. Low speed characteristics corresponding to incompressible flow conditions have been shown to collapse onto a single line (Courty-Audren et al., 2013). With knowledge of the windmilling point, the collapsed low speed characteristic could be interpolated to read the sub-idle portion of the map as shown in figure 1.

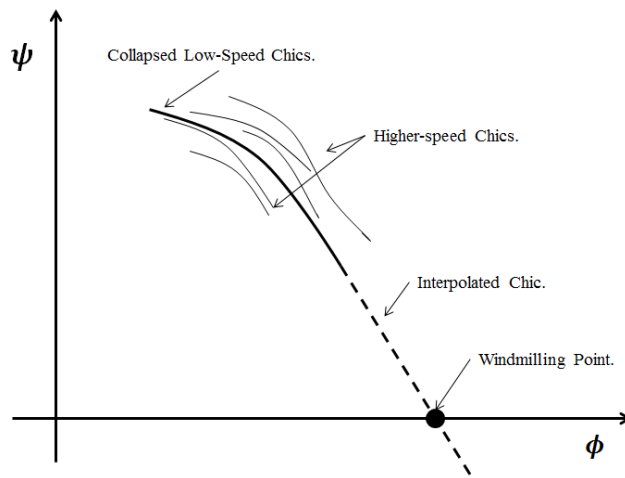


Figure 1 Conceptual use of windmilling point for sub-idle map generation using linearized parameters.

This procedure does not get rid of the issue at zero speed previously discussed. If the map is to be generated down to zero speed, then the corrected mass flow, speed, pressure ratio and torque parameters must be used, however, the possibility of using an analytically calculated windmilling point for map generation has the potential to increase the fidelity of the methods proposed.

EXPERIMENTAL TEST-BENCH

A Rolls-Royce Allison Model 250 (M250) C20b axial compressor assembly is used for this investigation. The M250 compression system consists of a six-stage axial compressor assembly followed by a centrifugal compressor. In this investigation, only the axial compressor assembly is used. In order to adapt the axial compressor assembly for use in a rig, a mating stub shaft transitions from the axial compressor hub to an auxiliary shaft used for adaption of a torque transducer. A constant annulus area is provided for pressure measurements. A bearing and bearing housing are manufactured to ensure proper axial alignment of the rotor within the assembly. The assembly was balanced at Rolls-Royce Bristol and delivered to Cranfield University.

The M250 axial compressor rig includes the instrumentation required for obtaining the pressure ratio and mass flow at all operating points as well as torque during locked rotor and shaft speed during windmill. The flow is generated via a downstream extraction fan and controlled via a butterfly valve. The extraction fan has a static pressure rating of 50 in.Wc (12.4 kPa) and capacity of 44 m³/min. A bell mouth and diffuser are used to deliver air to the compressor assembly front instrument casing. An image of the rig arrangement is shown in figure 2.

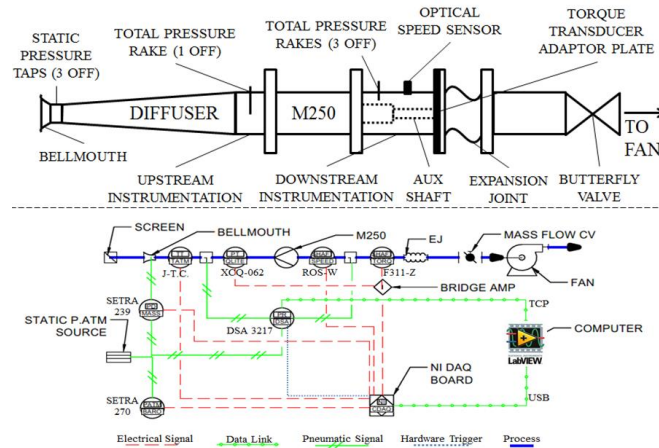


Figure 2 Experimental rig arrangement.

Two dedicated pressure transducers are used to determine the static pressure drop across the inlet bell mouth and the atmospheric pressure. From these measurements the mass flow into the rig is calculated. Three static pressure taps are taken at the bell mouth throat and pneumatically averaged. All ambient pressure readings, including the reference pressures, are measured from an ambient static chamber to ensure a stable reference atmosphere.

Total pressure readings for the determination of total pressure are taken with a Scanivalve pressure scanner. A total of nine individual pressure readings are taken at the compressor outlet, with five other readings taken at the compressor inlet. From these measurements, the total pressure ratio is calculated. The total pressure readings are taken using specially designed Kiel probes with 20 degrees of yaw sensitivity. Kiel probe yaw position is calibrated for maximum pressure recovery at each operating point measured. The pressure scanner used is bidirectional 5 psid [34.5 kPa]. A Novatech bespoke torque transducer is used to lock the compressor shaft for locked rotor studies. The transducer is placed on an adaptor plate and a groove in a compressor shaft extension allows the coupling of the transducer as shown in figure 3. The torque transducer and pressure scanner ranges were selected based on 3D CFD studies of the multistage compressor at sub-idle.

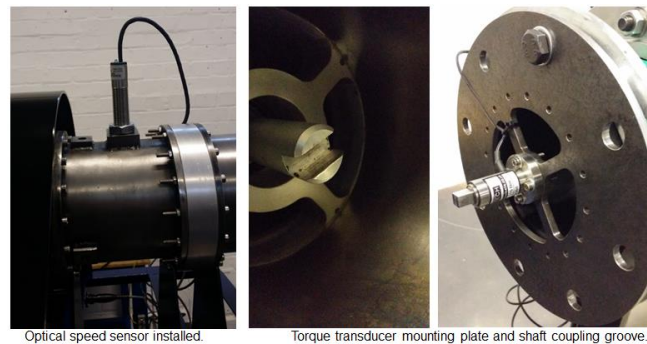


Figure 3 Speed sensor (left), torque transducer coupling shaft (center), and torque transducer (right).

The shaft speed is measured via a Monarch Instruments optical speed sensor and National Instruments digital counter. The optical sensor reads off a reflective sticker placed on the shaft extension. Data acquisition is done via a National Instruments DAQ board and LabVIEW Virtual Instrument. A bridge amplifier is used for the torque transducer. The pressure scanner interfaces directly to the data acquisition computer via a TCP Ethernet connection.

RESULTS & DISCUSSION

Pressure ratio characteristics have been obtained for both the locked rotor and windmilling cases. In addition, a torque characteristic is obtained for the locked rotor case while a shaft speed vs. corrected mass flow line is obtained for the windmilling case. Data is gathered at each mass-flow point using 1 minute sample times and a 5 Hz sampling rate, resulting in 300 samples per operating point. Error bars report combined standard uncertainty, including propagated instrumentation uncertainty and standard error of the mean at each point. A series of locked rotor and windmilling mass-flow points have been selected using the rig's butterfly valve. The mass flows tested are shown in table 1.

Table 1 Experimental cases

| Case | Normalized corrected mass flow (% of design point mass flow) |
|------|--|
|------|--|

| | | | | | | | | |
|---------------------|-----|-----|-----|-----|-----|------|------|------|
| Locked Rotor | 0.0 | 1.3 | 2.5 | 3.9 | 5.2 | 6.3 | 7.6 | 9.4 |
| Wind-milling | 2.0 | 4.0 | 5.4 | 7.3 | 9.3 | 11.3 | 12.6 | 14.3 |

Maximum mass flow achievable was limited by losses and the static pressure rating of the fan. The fan is not capable of delivering more flow when the maximum static pressure drop is reached. Lower pressure losses in the windmilling regime result in greater mass flow capability for the same static pressure rating on the extraction fan.

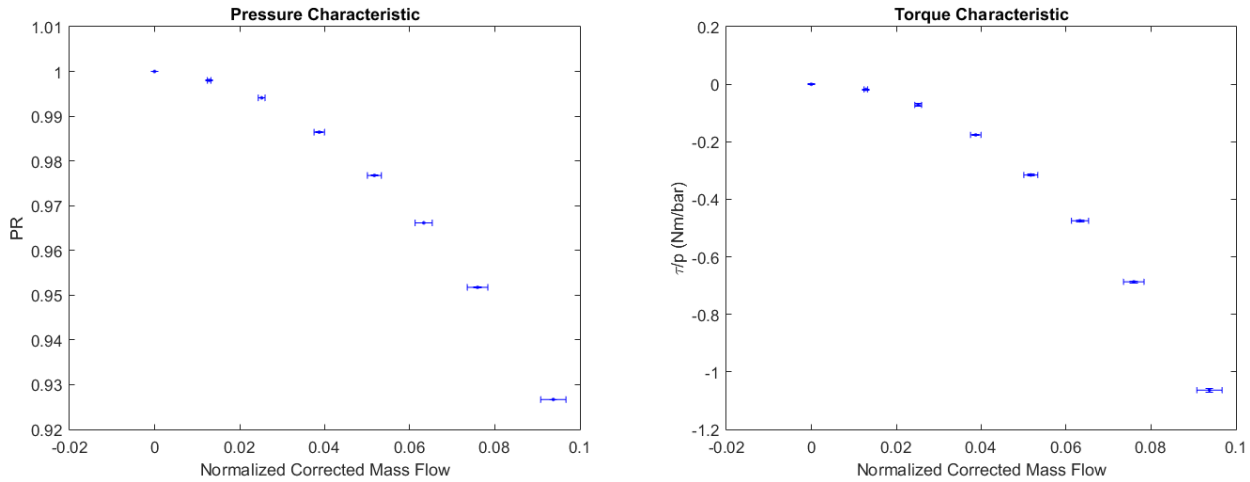
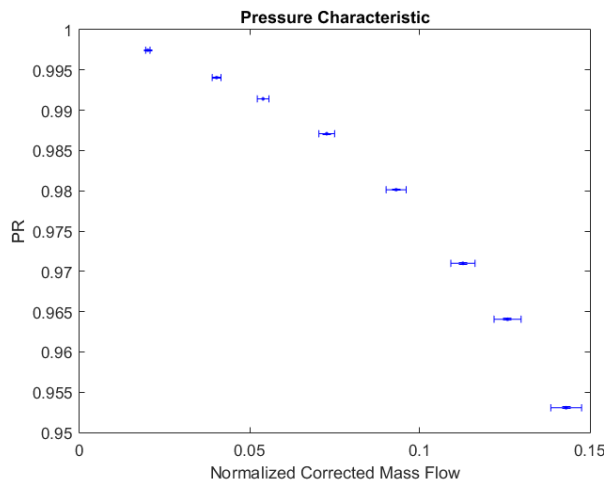


Figure 4 Experimental pressure and torque characteristics for locked rotor case.

The locked rotor characteristics in figure 4 follow the expected trends, with increasing pressure loss through the compressor as mass flow is increased. This is due to the compressor acting as a duct with obstacles in the form of cascade blade rows. The blades are expected to be experiencing large separation wakes while operating at high negative incidences. As mass flow increases, so too does the torque experienced on the shaft. Torque is considered negative in the locked rotor operation, as it is the working fluid which imparts a force on the blading and not in the opposite fashion, as would be expected of a compressor in normal operation.

Windmill results shown in figure 5 also show expected trends, with windmill shaft speed and pressure loss increasing as the mass flow is increased. An important aspect to highlight is the straight line relationship occurring between shaft speed and mass flow. The data presented here would suggest that a linear relationship between mass flow and speed, as has been discussed in the literature for fans, is also present in the case of multistage compressors, allowing the use of the windmilling line for map generation as previously discussed. The non-zero mass flow x-intercept apparent from figure 5 can be explained by non-negligible friction acting on the shaft at very low mass flows. A certain mass flow needs to be established before the shaft can beat the static friction and accelerate to a steady state.



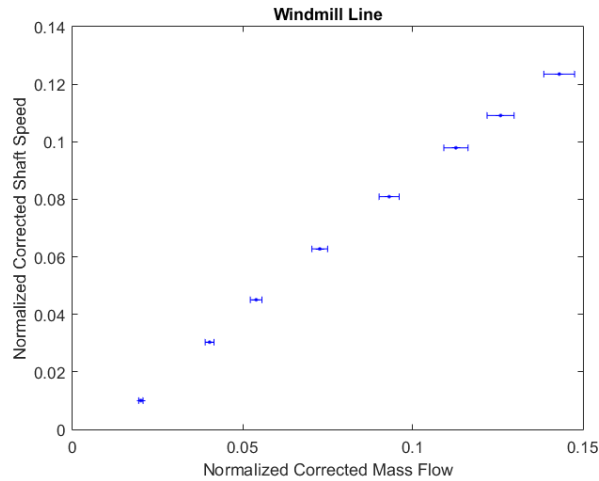


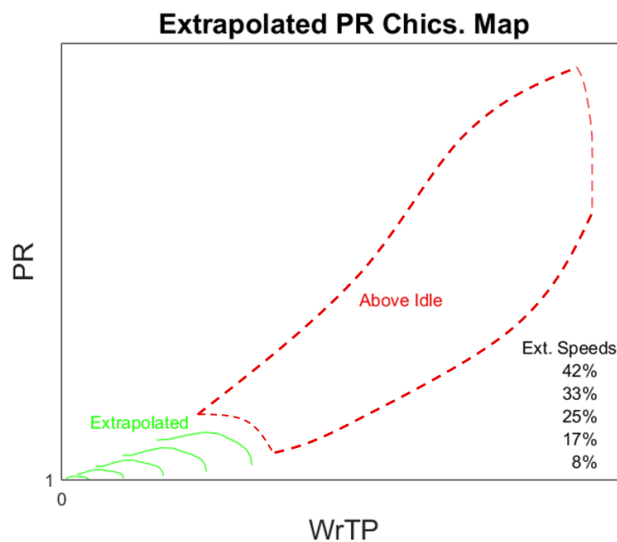
Figure 5 Experimental pressure characteristic and windmilling line for windmilling case.

MAP GENERATION

Component performance maps used within performance codes rely on beta-lines (sometimes called R-lines) to arrange the data in tables amenable to interpolation. In this manner, each beta-line contains a monotonically ordered set of performance data (Riegler, 2001). The lines resemble operating lines, but are entirely unphysical constructs used simply for ease of manipulation and data storage. The concept of beta-lines is more closely discussed in (Jones et al., 2001). These beta-lines are a fundamental concept used in the extrapolation and interpolation methodologies discussed below.

Interpolation vs. extrapolation

The extrapolation method by Gaudet & Gauthier (Gaudet and Gauthier, 2007) previously discussed is a strong candidate for testing against sub-idle data generated experimentally. Such a method resulted in promising results when tested against data generated down to 15% speed with an Allison M250-C20b in the work of Honle et al. (Honle et al., 2013). In that work, the axial-centrifugal compressor assembly was used, while only the axial compressor of the same model engine is used in the present work. Using this extrapolation procedure, the M250 compressor map down to idle is generated as shown in figure 6. In order to safeguard proprietary information, the M250 above-idle characteristics have been replaced with representative sketches showing the relative size of each map region. The sub-idle characteristics generated in this investigation have not been altered.



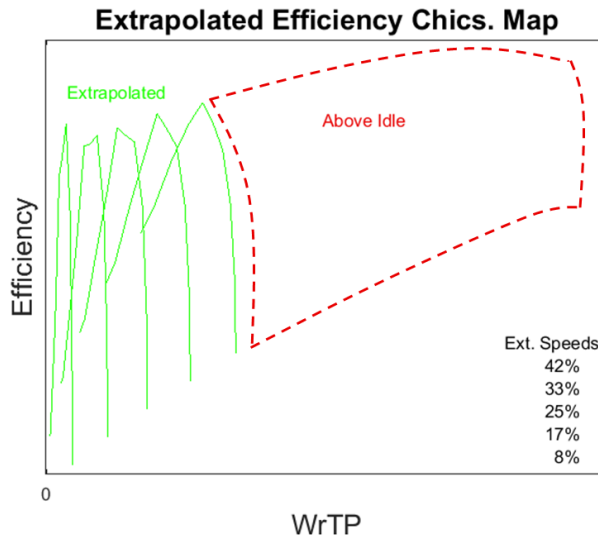


Figure 6 Extrapolated M250 axial compressor characteristics using the method in (Gaudet & Gauthier, 2007), with representative above-idle map.

The main advantage of such an extrapolation methodology is its simplicity, as only knowledge of two near-idle speed lines is required to obtain the sub-idle portion of the map by the application of the similarity laws. The maps obtained in this manner appear viable, especially near the idle region, and have been found to match experimental results for points not too far below idle in (Honle et al., 2013). However, there are two aspects which do not appear realistic, especially as shaft speed decreases:

1. The extrapolation process will always yield pressure ratios above unity, even for the locked rotor case.
2. Efficiency values always remain above zero, even for the locked rotor case, with surprisingly high peak efficiency values occurring at very low speeds.

Point one is clearly suspect, as we know that the overall pressure ratio must be below unity in the locked rotor case due to all blade rows being locked in place and acting as a cascade. Point 2 is also suspicious, as the efficiency would only be defined for those points where enthalpy is added to the flow. We know the windmilling line is the border between work addition and extraction (Zachos et al., 2011), and that efficiency becomes undefined at windmilling and below.

For these reasons, the sub-idle interpolation methodology presented in (Zachos et al., 2011) appears to be a good candidate for improved map physicality. The original interpolation methodology calls for the locked rotor line to be analytically calculated and then used for interpolation up to idle. In the current case, the locked rotor data gathered experimentally is used for interpolation. A Piecewise Cubic Hermite Interpolating Polynomial (PCHIP) is used to interpolate between the locked rotor and idle lines on each beta line. Such an interpolating approach ensures a shape-preserving interpolation. PCHIP interpolation ensures monotonicity and continuous first derivatives but not second derivatives, avoiding the overshoots and oscillations that could arise from spline interpolation. The sub-idle map generated in this manner is compared to the one generated using the Gaudet and Gauthier extrapolation method in figure 7.

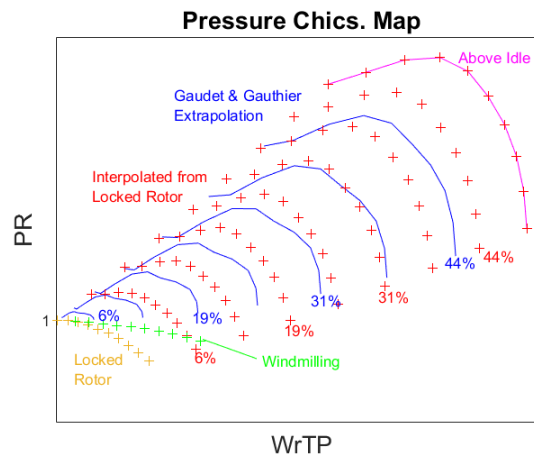


Figure 7 Comparison of interpolation and extrapolation methods for M250 sub-idle map.

As seen in fig 7, the lines generated by both methods clearly differ. While characteristics may seem qualitatively similar near idle, albeit offset from each other, the differences become more dramatic as we approach the locked rotor line. Predictably, the extrapolation method is unable to predict pressure ratios below unity, resulting in unrealistic characteristics being generated at very low speeds, which fail to capture the region of the experimentally generated windmilling line along with the correct speed-flow relationship. Due to the inability of dissipative losses to be characterized via extrapolation, the windmilling line falls completely outside the extrapolated map. The interpolated map does however allow for this region to be captured in a more realistic manner.

At this stage, the interpolation appears superior at low speed, but the accuracy of the interpolated characteristics must still be assessed. The points at which the windmilling line crosses the interpolated characteristics can be used to check the interpolation. The windmilling line must cross the interpolated characteristics where the speed of the characteristic matches the steady-state windmilling speed. This check is performed in figure 8. As it can be observed, the windmilling speeds appear grossly off the mark.

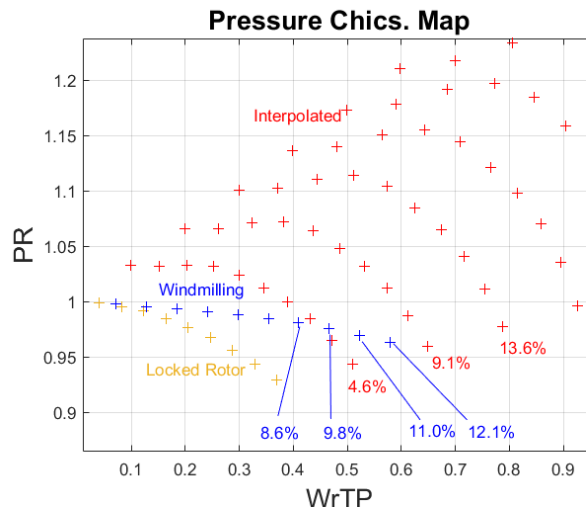


Figure 8 Interpolated low speed characteristics and experimental windmilling line.

While the interpolation method yields low speed characteristics that appear viable, these characteristics do not align properly with the captured windmilling data. This is likely the result of the interpolation method being agnostic to the change in operational regime (from compression to expansion) that occurs at the windmilling line. This change in the mode of operation can be expected to affect the shape of the characteristics; as the compressor is caused to effectively operate like a different device, namely a turbine.

Use of the windmilling line

While the interpolation method characterizes low speed operation more closely than an extrapolation approach for this compressor, the accuracy of the interpolated characteristics remains to be improved. In an attempt to improve this accuracy, the windmilling data is used within the interpolation. In such a method, the windmilling points are introduced into the beta-lines to be interpolated along with the locked rotor data. After carrying out this interpolation, the low-speed map in figure 9 results.

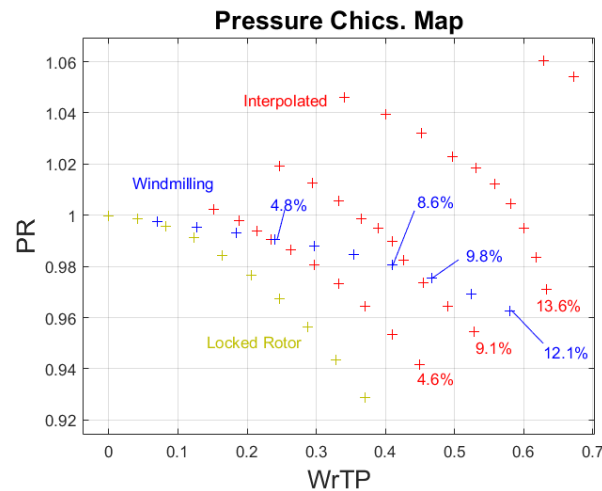


Figure 9 Interpolated low speed characteristics using windmilling line.

The addition of the windmilling line into the interpolation procedure steepens the characteristics so that the windmilling speeds match the appropriate constant-speed lines. As seen in figure 9, this greatly affects the shape and location of these lines near zero speed. The full sub-idle map generated in this manner is shown in figure 10 and compared to the one generated via interpolation only from locked rotor.

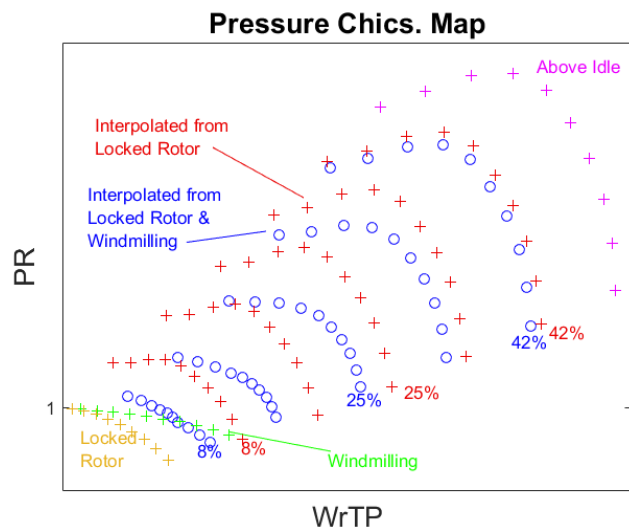


Figure 10 Comparison of interpolation methods.

The compressor maps generated using this procedure are shown in figure 11, including the torque parameter. As before, representative above-idle maps have been included in these figures to show the relative size of each map region while safeguarding proprietary information.

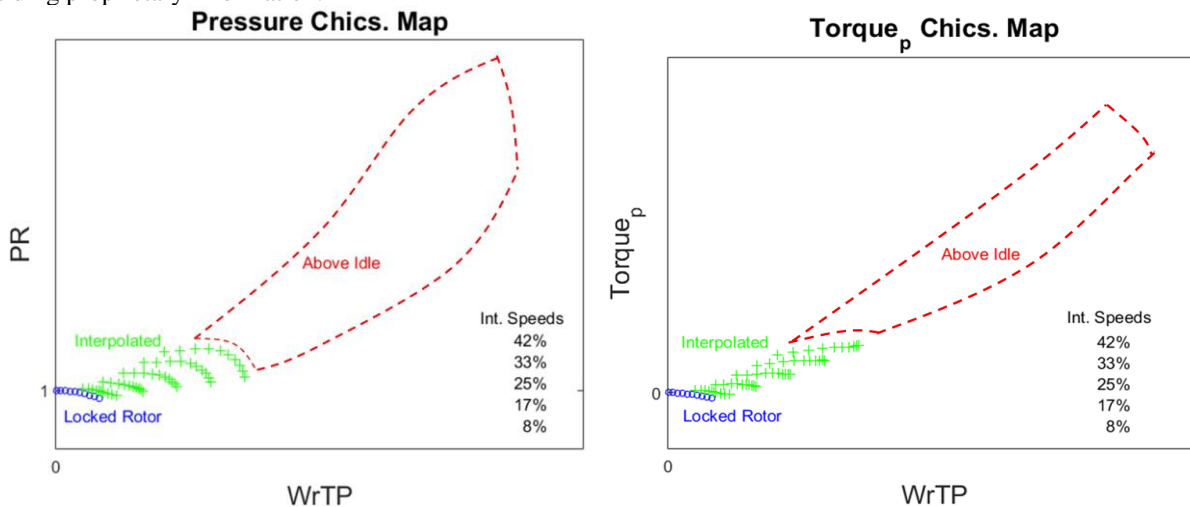


Figure 11 M250 maps after interpolation using windmilling line and representative above-idle map.

The maps generated allow the sub-idle portion to be included in performance calculations so that start-up and windmill-to-relight events can be simulated. The addition of the windmilling characteristic ensures that simulations at the very low-speed portions of the map accurately represent the physics of operation in the windmill and turbine operating regions.

The algorithms used to generate the above maps automatically generate arrays organizing the information in terms of beta-lines to make the map data amenable to performance prediction tools. A performance code using this sub-idle data would need to be modified to use the torque parameter instead of efficiency, but this can be accomplished via equation (5) and has been previously demonstrated by (Grech, 2013).

CONCLUSIONS

An experimental sub-idle rig has been designed, built and commissioned using a Rolls-Royce Allison Model 250-C20b axial compressor assembly. The rig has been used to generate locked-rotor and windmilling data in the form of pressure and torque characteristics. Locked rotor data follows expected trends with losses and shaft torque increasing with mass flow in a quadratic

fashion. Windmilling data shows evidence of a linear relationship between mass flow and shaft speed, as has been previously discussed in the literature for the case of single stage fans.

The experimental data has been used to generate compressor maps down to idle speed using an interpolation methodology. The generated maps have been compared to an existing extrapolation technique showing how interpolation from the locked rotor line yields maps that more closely match the physics expected. However, interpolation from the locked rotor line alone does not adequately capture the windmilling region in this compressor. The addition of the windmilling characteristic for interpolation is shown to increase the accuracy of the speed lines generated and is recommended by these authors as an important correction to the interpolation process. Use of the windmilling characteristic to aid map generation into the sub-idle region is hitherto unknown to the authors.

In order to use the windmilling characteristic for map generation, prior knowledge of the windmilling point is needed. A robust analytical method for obtaining locked rotor and windmilling lines, or even a simple method for predicting the windmilling speed, would result in a noticeable improvement in the map generation process. Methods to predict windmilling mass flows, pressure losses, and speeds for single stage fans have already been highlighted in the literature. The linear relationship between windmilling mass flow and shaft speed seen for this compressor suggests that similar methods may be applicable to multistage compressors. Developing windmilling point prediction methods for multistage compressors has the potential to greatly improve the sub-idle map generation process.

NOMENCLATURE

| | |
|------------------|---|
| Δh | Specific stagnation enthalpy change [kJ/kg] |
| \dot{m}_{corr} | Corrected mass flow [kg/s] |
| N | Percent shaft speed [%] |
| P | Pressure [Pa] |
| PR | Total pressure ratio |
| p, q, r | Extrapolation exponents |
| T | Temperature [K] |
| U | Blade speed [m/s] |
| V_{ax} | Axial velocity [m/s] |
| $WrTP$ | Flow function [$lb\sqrt{K}/psia$] |
| γ | Adiabatic coefficient |
| ϕ | Flow coefficient |
| ψ | Work coefficient |
| Π_0 | Total pressure ratio |
| η_x | Isentropic efficiency |
| τ | Torque [Nm] |

Subscripts

| | |
|------------|--|
| $in, 1, 2$ | Compressor stations |
| is | Isentropic |
| ref | Reference speed line or reference conditions |
| $ref + 1$ | Next speed line above reference |
| tot | Stagnation conditions |
| x | Relating to a specific speed line |

ACKNOWLEDGEMENTS

The authors would like to thank Rolls-Royce plc. for making this research possible and allowing its publication. The authors would also like to thank Peter Calvert, Matt Hollins, Jason Lee, and Sarah Terry, the Rolls-Royce Design & Make team originally tasked with sourcing, designing and preparing the M250 axial compressor rig for integration into an experimental test bench at Cranfield University.

REFERENCES

- [1] Agrawal, R. K., and M. Yunis. (1982). A generalized mathematical model to estimate gas turbine starting characteristics. Transactions of the ASME 104, pp. 194-201.
- [2] Aslanidou, I., Zachos, P. K., Pachidis, V., Singh, R. (2010). A physically enhanced method for sub-idle compressor map generation and representation. ASME. Turbo Expo 2010, doi:10.1115/GT2010-23562.
- [3] Audren, C., Kee, S., Carbonneau, X., Binder, N., and Florent, C. (2013). Potential of power recovery of a subsonic axial fan in windmilling operation. 10th European Turbomachinery Conference.

- [4] Binder, N., Courty-Audren, S.-K., Duplaa, S., Dufour, G., and Carbonneau, X. (2015). Theoretical analysis of the aerodynamics of low-speed fans in free and load-controlled windmilling operation. *ASME Journal of Turbomachinery*, 137(10), doi: 10.1115/1.4030308
- [5] EASA (2015). Certification Memorandum: Turbine Engine Relighting In Flight, Pub. L. No. CS-E 910, 1
- [6] Farokhi, S. (2014). *Aircraft propulsion*. (2nd ed). Wiley, doi: 10.2514/1.J054236
- [7] Gaudet, S. R., & Gauthier, J. E. D. (2007). A simple sub-idle component map extrapolation method. *ASME Turbo Expo 2007*, doi:10.1115/GT2007-27193
- [8] Grech, N. (2013). Gas turbine sub-idle performance modelling; groundstart, altitude relight and windmilling. PhD Thesis, Cranfield University.
- [9] Honle, J., Kerler, M., Nachtingall, H., Erhard, W., and Kau, H. (2013). Experimental validation of a sub-idle compressor map extrapolation. *ISABE 2013*.
- [10] Howard, J. (2007). Sub-idle modelling of gas turbines; altitude relight and windmilling. PhD Thesis, Cranfield University.
- [11] Illana, E., Grech, N., Zachos, P. K., & Pachidis, V. (2013). Axial compressor aerodynamics under sub-idle conditions. *ASME Turbo Expo 2013*.
- [12] Jia, L., and Chen, Y. (2016). Validation of a physically enhanced sub idle compressor map extrapolation method. *International Symposium on Transport Phenomena and Dynamics of Rotating Machinery 2016*.
- [13] Jones, G., Pilidis, P., and Curnock, B. (2001). Compressor characteristics in gas turbine performance modelling. *ASME Turbo Expo 2001*.
- [14] Kurzke, J. (1996). How to get component maps for aircraft gas turbine performance calculations. *International Gas Turbine and Aeroengine Congress and Exhibition* (pp. 1–7).
- [15] Riegler, C., Bauer, M., and Kurzke, J. (2001). Some aspects of modeling compressor behavior in gas turbine performance calculations. *ASME Journal of Turbomachinery*.
- [16] Sexton, W. R. (2001). A method to control turbofan engine starting by varying compressor surge valve bleed. MS Thesis, Virginia Polytechnic Institute and State University.
- [17] Walsh, P. and Fletcher, P. (2004). *Gas Turbine Performance*, (2nd ed). Oxford, UK: Blackwell Science.
- [18] Zachos, P. K., Aslanidou, I., Pachidis, V., and Singh, R. (2011). A sub-idle compressor characteristic generation method with enhanced physical background. *ASME Journal of Engineering for Gas Turbine and Power* 133, doi: 10.1115/1.4002820
- [19] Zachos, P. K. (2013). Modelling and analysis of turbofan engines under windmilling conditions. *ASME Journal of Propulsion and Power*, 29(4), 882–890., doi: 10.2514/1.B34729